ACS Medicinal Chemistry Letters

Letter

Cite This: ACS Med. Chem. Lett. 2018, 9, 730−735

Optimization of ZD2 Peptide Targeted Gd(HP-DO3A) for Detection and Risk-Stratification of Prostate Cancer with MRI

Nadia R. Ayat,[†,§] Jing-Can Qin,[†,§] Han Cheng,[†] Sarah Roelle,[†] Songqi Gao,[†,‡] Yajuan Li,[‡] and Zheng-Rong Lu*[,†]

[†]Case Center for Biomolecular Engineering, Department of Biomedical Engineering, School of Engineering, Case Western Reserve University, Cleveland, Ohio 44106, United States

[‡]Molecular Theranostics, Cleveland, Ohio 44115, United States

Supporting Information

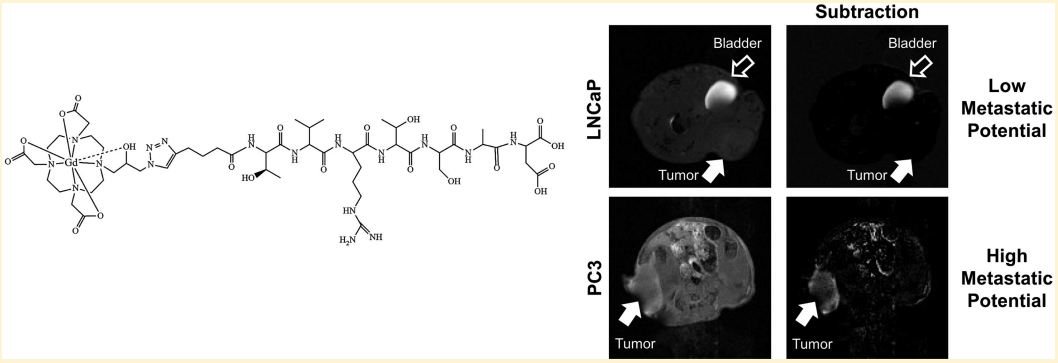

ABSTRACT: The aim of this work is to optimize a peptide targeted macrocyclic MRI contrast agent for detection and risk-stratification of aggressive prostate cancer. The optimized agent was prepared using click chemistry in the presence of $CuSO_4$ and ascorbate at room temperature. The T_1 and T_2 relaxivities of ZD2-N3-Gd(HP-DO3A) are 5.44 and 7.10 mM^{-1} s^{-1} at 1.4 T, and 5.53 and 7.81 mM^{-1} s^{-1} at 7 T, respectively, higher than the previously reported ZD2-Gd(HP-DO3A). The specific tumor enhancement of the agent was investigated in male nude mice bearing aggressive PC3 human prostate cancer xenografts and slow-growing LNCaP tumor xenografts. Contrast enhanced MR images were acquired using a 2D spin−echo sequence and a 3D FLASH sequence with a 7 T small animal scanner. ZD2-N3-Gd(HP-DO3A) produced robust contrast enhancement in aggressive PC3 tumors and little enhancement in slow-growing LNCaP tumors. It produced 400% and 100% CNR increases in the T_1-weighted 2D spin−echo MR images and 3D FLASH images of PC3 tumors, respectively, for at least 30 min at a dose of 0.1 mmol/kg. In contrast, less than 20% CNR increase was observed in the LNCaP tumors with both sequences. The optimized targeted contrast agent has higher relaxivities and are effective to detect aggressive PC3 tumors and differentiate the aggressive cancer from the slow-growing LNCaP prostate cancer in contrast enhanced MRI. ZD2-N3-Gd(HP-DO3A) has the promise for accurate detection and risk-stratification of aggressive prostate cancer.

KEYWORDS: *ZD2 peptide, EDB fibronectin, targeted MRI contrast agent, prostate cancer, cancer detection and risk-stratification*

Prostate cancer is a heterogeneous disease with high incidence in men over the age of 50. Approximately 30% of patients diagnosed with prostate cancer may die from the disease. Current diagnostic methods for prostate cancer suffer from high rates of overdiagnosis, which often leads to unnecessary overtreatment and unintended side effects.[1−3] Accurate early detection and risk-stratification of the disease is critical to tailor patient-based therapies to improve the healthcare of prostate cancer patients. Molecular imaging provides noninvasive measurement and visualization of oncogenic biomarkers and gives the potential for accurate cancer detection and risk-stratification of malignant tumors. Magnetic resonance imaging (MRI) is commonly used for detection and characterization of prostate cancer and for decision-making in the healthcare of patients.[4,5] Contrast agents based on small molecular Gd(III) chelates are routinely used to enhance image contrast in cancer MRI.[6] However, these contrast agents are nonspecific and unable to provide accurate detection and risk-stratification of the disease. There is an unmet clinical need of safe and effective contrast agents specific to oncotargets for high-resolution MR molecular imaging (MRMI) and accurate detection and risk-stratification of prostate cancer.

Advancements in cancer biology have highlighted the importance of the tumor microenvironment for cancer aggressiveness, progression, and metastasis. A major compo-

Received: April 12, 2018
Accepted: June 6, 2018
Published: June 6, 2018

DOI: 10.1021/acsmedchemlett.8b00172
ACS Med. Chem. Lett. 2018, 9, 730−735

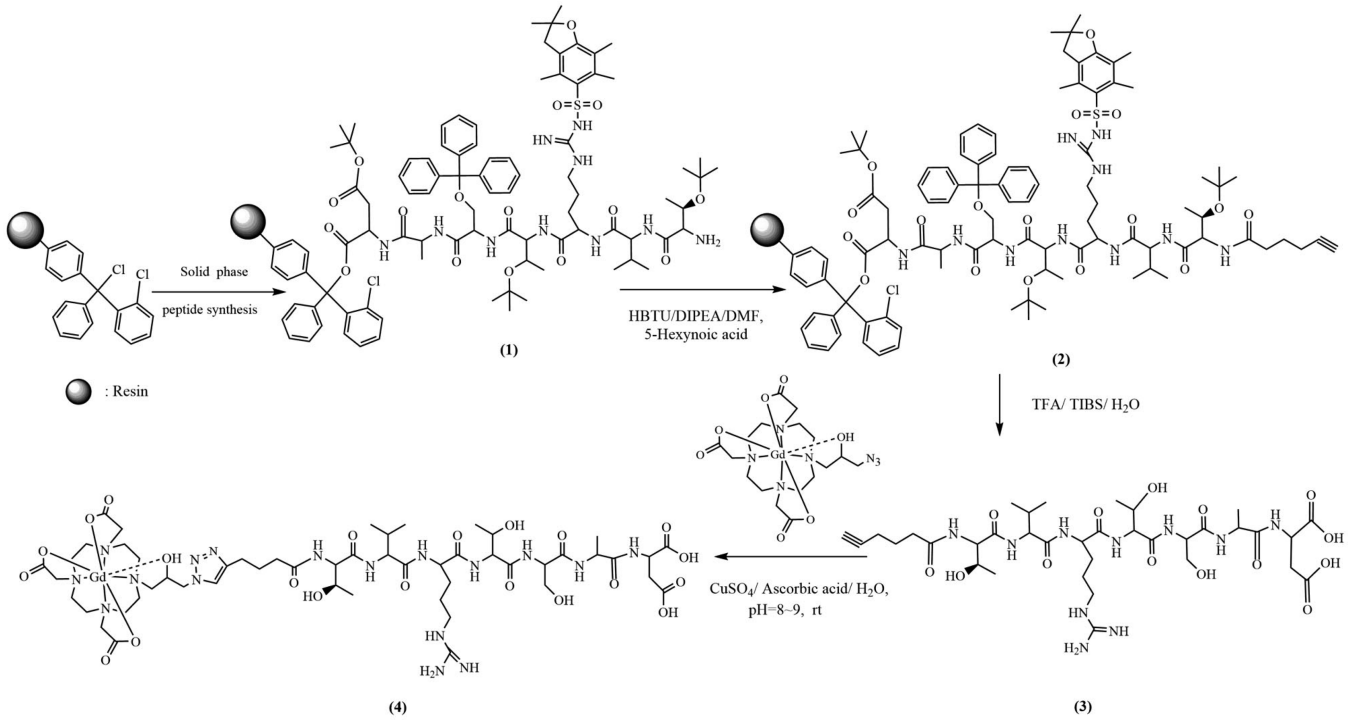

Figure 1. Chemical synthesis of ZD2-N3-Gd(HP-DO3A).

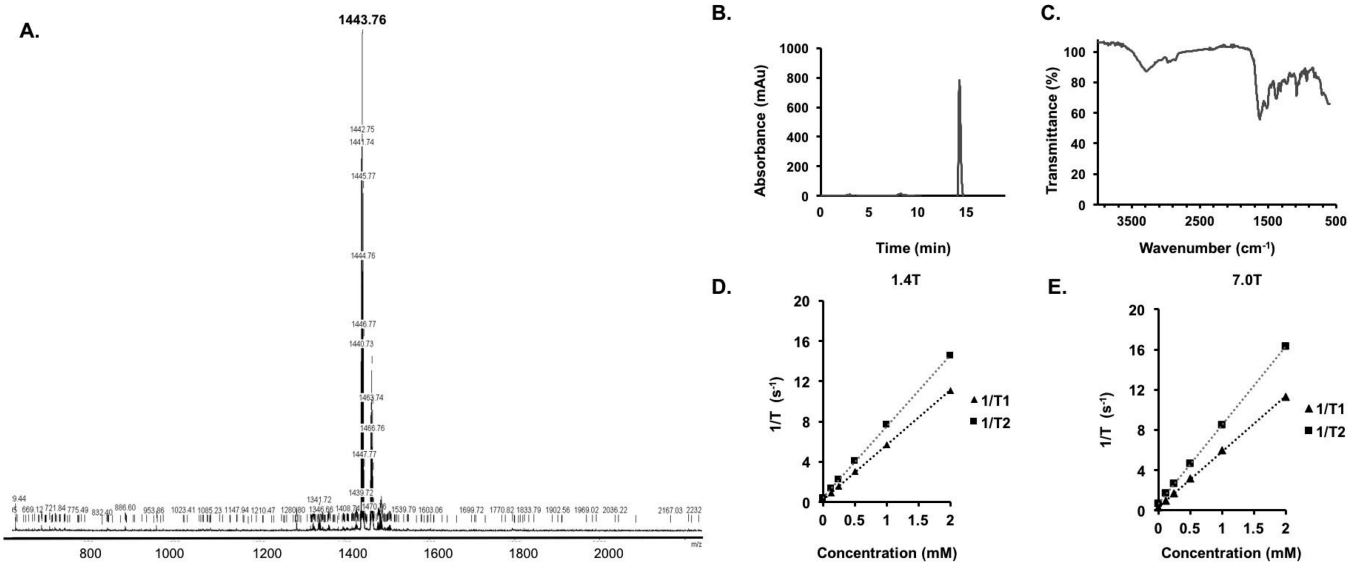

Figure 2. Characterization of ZD2-N3-Gd(HP-DO3A). (a) MALDI-TOF spectrum of ZD2-N3-Gd(HP-DO3A). (b) HPLC spectrum of ZD2-N3-Gd(HP-DO3A). (c) IR spectrum of ZD2-N3-Gd(HP-DO3A). (d) $1/T_1$ and $1/T_2$ measured with phantoms of various concentrations of ZD2-N3-Gd(HP-DO3A) at 1.4T at 37 °C. (e) Plot of $1/T_1$ and $1/T_2$ measured with phantoms of various concentrations of ZD2-N3-Gd(HP-DO3A) at 7.0 T. Relaxivity was calculated as the slope of $1/T$ vs concentration.

nent of the tumor microenvironment is the extracellular matrix (ECM), which consists of highly deregulated components when compared to normal tissue. Extradomain-B fibronectin (EDB-FN) is highly expressed in the tumor extracellular matrix of aggressive tumors when compared to normal tissues.[7−9] EDB-FN expression in tumor ECM has been associated with poor prognosis in cancers, thus making it a promising target for molecular imaging and precision medicine. We have developed a peptide specific to EDB-FN, named ZD2 (Cys-Thr-Val-Arg-Thr-Ser-Ala-Asp).[10] We have also developed targeted MRI contrast agents by conjugating this peptide to macrocyclic clinical contrast agents and Gd_3N@C80.[11−13] The agents can bind to abundant EDB-FN in aggressive tumors to generate robust signal enhancement for detection and risk-stratification of aggressive cancer, including breast and prostate cancers with MRMI.[13,14]

To identify a suitable targeted MRI contrast agent for clinical translation, we sought to optimize the structure and synthesis of the previously reported ZD2-Gd(HP-DO3A).[13] It was synthesized by a click reaction at high temperature for long reaction time, which may cause peptide degradation. We also thought that removal of the flexible short PEG spacer in ZD2-

DOI: 10.1021/acsmedchemlett.8b00172
ACS Med. Chem. Lett. 2018, 9, 730−735

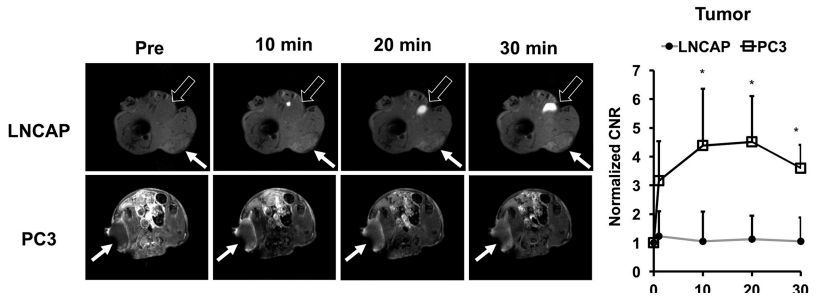

Figure 3. Representative T_1-weighted axial 2D spin echo MR images (A) and CNR (B) of LNCaP and PC3 bearing mice at 0.1 mmol Gd/kg of ZD2-N3-Gd(HP-DO3A) (n = 4). Tumors are indicated by the solid arrows (n = 4) (*p < 0.05), whereas the bladder is indicated by the hollow arrow.

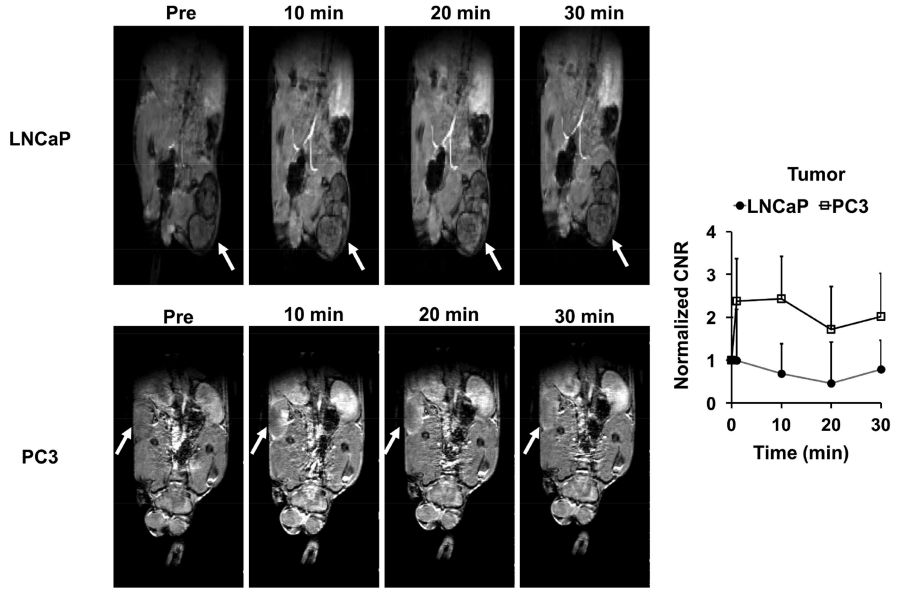

Figure 4. T_1-weighted FLASH coronal MR images of LNCaP (A) and PC3 (B) bearing mice injected with ZD2-N3-Gd(HP-DO3A) at 0.1 mmol Gd/kg (n = 4). Tumors are indicated by the arrows. (C) CNR in the tumors with ZD2-N3-Gd(HP-DO3A) and the 3D FLASH sequence.

Gd(HP-DO3A) could improve the relaxivities by increasing molecular rigidity. Here, we optimized the structure of the ZD2 peptide Gd(HP-DO3A) conjugate by removing the PEG spacer to give ZD2-N3-Gd(HP-DO3A). The reaction condition for click reaction was also optimized to allow the synthesis to be performed in aqueous solution at room temperature. The efficacy of ZD2-N3-Gd(HP-DO3A) for MRMI, detection, and risk-stratification of prostate cancer was investigated in male nude mice bearing aggressive and fast-growing PC3 and slow-growing LNCaP prostate cancer xenografts.

The synthetic procedure of the optimized contrast agent ZD2-N3-Gd(HP-DO3A) is shown in Figure 1. ZD2 peptide was synthesized using solid phase chemistry as previously described.[10,13] The product was characterized by MALDI-TOF mass spectrometry, m/z (M + 1): 843.57; 843.413. (calc.). The azido-containing macrocyclic Gd(III) chelate, N3-Gd(HP-DO3A), was prepared according to a published method.[15] The click reaction between alkynyl-ZD2 and N3-Gd(HP-DO3A) was performed in aqueous solution without nitrogen protection at room temperature. The catalyst $[Cu(MeCN)_4]$-PF6 and TBTA (tris[(1-benzyl-1*H*-1,2,3-triazol-4-yl)-methyl]-amine) was replaced with inexpensive $CuSO_4$ and ascorbate. Alkynyl-ZD2 (0.40 mmol) and N3-Gd(HP-DO3A) (0.60 mmol) were dissolved in 25 mL of deionized water. $CuSO_4$ (1.6 mL, 0.05 N) and ascorbic acid (5 mL, 0.05 N in water) were added, the pH of solvent was adjusted to 8−9 by 0.1 N NaOH, and the mixture was stirred at room temperature for 24 h. The product was purified by FLASH chromatography (yield: 40%). The final product ZD2-N3-Gd(HP-DO3A) was characterized by MALDI-TOF mass spectrometry, m/z (M + H^+) 1443.73; 1443.54 (calc.), Figure 2A. The high purity of the final product also was confirmed by HPLC, Figure 2B. The infrared spectrum of ZD2-N3-Gd(HP-DO3A) is shown in Figure 2C and shows characteristic peaks (cm^{-1}) at 3280 (σ_{O-H} and σ_{N-H}), 2968 (σ_{C-H}), 2925 (σ_{C-H}), 1625 ($\sigma_{C=O}$), 1518 ($\sigma_{C=N}$, $\sigma_{N=N}$, $\sigma_{C=C}$), 1385 (δ_{C-H}).

Plots of the longitudinal ($1/T_1$) or transverse ($1/T_2$) water relaxation rates versus the concentrations of the contrast agent at 1.4 and 7 T are shown in Figure 2D,E. The r_1 and r_2 relaxivities of ZD2-N3-Gd(HP-DO3A) are 5.44 and 7.10 mM^{-1} s^{-1} at 1.4 T, and 5.53 and 7.81 mM^{-1} s^{-1} at 7 T, respectively. ZD2-N3-Gd(HP-DO3A) has higher relaxivities than the previously reported ZD2-Gd(HP-DO3A) at both 1.4 and 7 T. The higher relaxivities of ZD2-N3-Gd(HP-DO3A) are attributed to the increased molecular rigidity after the removal of the flexible PEG spacer in ZD2-Gd(HP-DO3A). The increased molecular rigidity limits the motion of Gd(HP-DO3A) and increases the rotational time of the agent, resulting in higher relaxivities. Interestingly, ZD2-N3-Gd(HP-DO3A) exhibited a slightly higher relaxivity at 7 T than 1.4 T.

DOI: 10.1021/acsmedchemlett.8b00172
ACS Med. Chem. Lett. 2018, 9, 730−735

The ability of ZD2-N3-Gd(HP-DO3A) for differential contrast enhanced MRMI of prostate tumors of different aggressiveness was examined in mice bearing aggressive PC3 and slow-growing LNCaP human prostate cancer xenografts. T_1-weighted MR images were obtained before and after injection of 0.1 mmol/kg ZD2-N3-Gd(HP-DO3A) using 2D spin−echo and 3D FLASH sequences. Figure 3 shows axial 2D T_1-weighted spin−echo MR images of the mice bearing the prostate tumor xenografts. ZD2-N3-Gd(HP-DO3A) produced stronger signal enhancement in fast-growing PC3 tumors than the slow-growing LNCaP tumors. The strong signal enhancement in PC3 tumors sustained for at least 30 min post-injection. Subtraction of the precontrast images from postcontrast images provided a clear delineation of the PC3 tumor with strong enhancement, while the LNCaP tumors were not visible in the subtraction images. Contrast-to-noise ratio (CNR) in PC3 tumors increased 4-fold for at least 30 min post-injection. LNCaP tumors exhibited little increase in CNR. These results suggest that contrast enhanced MRI with ZD2-N3-Gd(HP-DO3A) can detect aggressive prostate cancer and differentiate between high and low risk prostate cancer tumors.

The effectiveness of the targeted contrast agent was also evaluated with a T_1-weighted 3D FLASH sequence in the tumor models. Figure 4 shows the 2D coronal images of the mice bearing the prostate tumor xenografts contrast enhanced by ZD2-N3-Gd(HP-DO3A). Significant enhancement in PC3 tumor was observed in 3D FLASH T_1-weighted images, with about 100% increase of CNR for at least 30 min post-injection. Only slight signal enhancement was observed in LNCaP tumors with little CNR increase. Figure 5 shows volume rendering maximum intensity projections (MIP) images of the tumor bearing mice at 30 min post-injection. Strong tumor enhancement was also highlighted in the MIP images of PC3 tumors with little accumulation in nonspecific tissue. Little signal enhancement was visible in the LNCaP tumor. Strong enhancement was also observed in the kidneys and bladder in the T_1-weighted FLASH images and MIP images, indicating the excretion of the unbound agent via renal filtration.

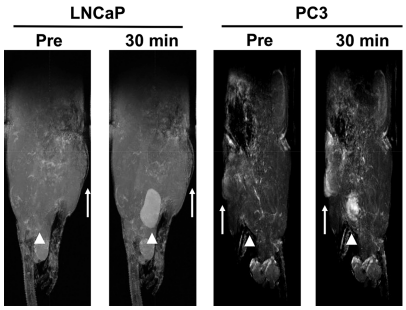

Figure 5. MIP volume rendering images were generated from T_1-weighted FLASH 3D coronal MR images of LNCaP and PC3 bearing mice. Tumors are indicated with arrows, and bladder is indicated by arrowheads.

Similar to ZD2-Gd(HP-DO3A), ZD2-N3-Gd(HP-DO3A) results in robust enhancement in PC3 tumors in T_1-weighted spin−echo images, with CNR increasing more than 4-fold. Significant signal enhancement was also generated in 3D FLASH images of the PC3 tumors with about 100% increase in CNR by the targeted agent. ZD2-N3-Gd(HP-DO3A) also shows good specificity with little signal enhancement in the slow growing tumor with low EDB-FN expression. The unbound ZD2-N3-Gd(HP-DO3A) can be readily excreted via renal filtration, which is critical to minimize long-term tissue accumulation of the gadolinium-based contrast agent. These results suggest structure modification of ZD2-N3-Gd(HP-DO3A) does not affect specific binding of the peptide to EDB-FN highly expressed in aggressive PC3 tumors. As shown in the previous study, ZD2-Gd(HP-DO3A) had similar tissue retention as a clinical contrast agent Gd(HP-DO3A) in mice. Since ZD2-N3-Gd(HP-DO3A) has a smaller molecular weight than ZD2-Gd(HP-DO3A), it is expected that ZD2-N3-Gd(HP-DO3A) will have a similar low tissue retention as the clinical agent.

The above work highlights the potential of targeted contrast agents to be utilized in the diagnosis and treatment planning of prostate cancer.[16,17] The potential of high-resolution MRMI has yet to be fully realized due to the lack of targeted contrast agents for aggressive prostate tumors.[18−21] Here, we have developed a targeted contrast agent specific to oncoprotein EDB-FN, a marker of epithelial-to-mesenchymal transition and highly expressed in aggressive prostate cancer and low in low-grade tumors.[7,9,10] Peptide targeted MRI contrast agents specific to EDB-FN have been developed for MRMI of aggressive cancers, including prostate cancer,[12−14] and have promise for accurate diagnosis of prostate cancer with MRMI.

Contrast enhanced MRI generally has a low sensitivity of molecular imaging of the biomarkers expressed on cancer cell surface because of low concentrations of these biomarkers. Targeted nanoparticles with a high payload of clinical contrast agents have been developed to increase the local concentration of the agent to generate detectable signal enhancement around the biomarkers in MRI.[22−24] Although these nanoparticle based targeted contrast agents are effective for specific tumor enhancement in animal tumor models, clinical translation of the nanosized agents are hindered by the safety concerns, especially for nephrogenic systemic fibrosis,[25−27] associated with their slow excretion. We have demonstrated that robust signal enhancement can be achieved by targeting the abundant extracellular matrix oncoproteins using small molecular targeted MRI contrast agents.[13,28,29] The ECM targets are easily accessible by the small molecular contrast agents by diffusion. A sufficient amount of the agents can bind to the targets to generate significant and prolonged tumor enhancement for effective molecular MRI across the tumor tissue. In contrast, tumor enhancement by nanosized targeted contrast agents generally restrain in the tumor rim due to limited penetration into inner tumor tissue. Our small molecular targeted contrast agents can be readily excreted from renal filtration, a major safety advantage over nanosized targeted contrast agent.

The targeted contrast agent is designed based on a clinical macrocyclic contrast agent Gd(HP-DO3A), which has shown high thermodynamic and kinetic stability and good safety profile in clinical practice.[30,31] The macrocyclic contrast agents also have low long-term brain accumulation as compared to the linear contrast agents.[32] It is expected that ZD2-N3-Gd(HP-DO3A) should have a similar safety property as the clinical macrocyclic agent. Nevertheless, comprehensive assessment of the physicochemical properties, pharmacokinetics, pharmacology, and toxicity of the agent is necessary to meet the requirements of regulatory agencies before clinical studies. Successful development of the targeted contrast agent will enable clinical MRMI of the entire prostate with high resolution and to address the unmet clinical need of noninvasive detection and risk-stratification of aggressive prostate cancer. High-

DOI: 10.1021/acsmedchemlett.8b00172
ACS Med. Chem. Lett. 2018, 9, 730−735

resolution MRMI with the targeted MRI contrast agent can provide early detection of aggressive tumors of microscopic sizes in the prostate. Early accurate detection and risk-stratification of aggressive prostate tumors will facilitate the decision-making in the disease management to initiate therapeutic interventions at a treatable stage. Clinical implementation of the imaging agent will also allow non-invasive active surveillance of low-grade prostate cancer, assessment of therapeutic efficacy, and image-guided interventions. This targeted contrast agent is promising for further clinical development to provide accurate detection and risk stratification of prostate cancer.

■ ASSOCIATED CONTENT

Supporting Information

The Supporting Information is available free of charge on the ACS Publications website at DOI: 10.1021/acsmedchemlett.8b00172.

Materials and methods (PDF)

■ AUTHOR INFORMATION

Corresponding Author

*E-mail: zxl125@case.edu. Phone: 216-368-0187.

ORCID

Zheng-Rong Lu: 0000-0001-8185-9519

Author Contributions

§These authors contributed equally.

Funding

This research was supported in part by the National Institute of Health grants R01CA194518 (to Z.R.L.) and R44CA199826 (to Y.L.).

Notes

The authors declare the following competing financial interest(s): Z.-R.L., Y.L., and S.G. are members of Molecular Theranostics, LLC, which is focused on the commercialization of targeted MRI contrast agents.

■ ACKNOWLEDGMENTS

Z.-R.L. is a M. Frank Rudy and Margaret Domiter Rudy Professor of Biomedical Engineering.

■ REFERENCES

(1) Sohn, E. Screening: Diagnostic dilemma. *Nature* **2015**, *528* (7582), S120−2.

(2) Heijnsdijk, E. A.; der Kinderen, A.; Wever, E. M.; Draisma, G.; Roobol, M. J.; de Koning, H. J. Overdetection, overtreatment and costs in prostate-specific antigen screening for prostate cancer. *Br. J. Cancer* **2009**, *101* (11), 1833−8.

(3) Glass, A. S.; Cary, K. C.; Cooperberg, M. R. Risk-based prostate cancer screening: who and how? *Curr. Urol Rep* **2013**, *14* (3), 192−8.

(4) Johnson, D. C.; Reiter, R. E. Multi-parametric magnetic resonance imaging as a management decision tool. *Transl Androl Urol* **2017**, *6* (3), 472−482.

(5) Hoffmann, M. A.; Taymoorian, K.; Ruf, C.; Gerhards, A.; Leyendecker, K.; Stein, T.; Jakobs, F. M.; Schreckenberger, M. Diagnostic Performance of Multiparametric Magnetic Resonance Imaging and Fusion Targeted Biopsy to Detect Significant Prostate Cancer. *Anticancer Res.* **2017**, *37* (12), 6871−6877.

(6) Zhou, Z.; Lu, Z. R. Gadolinium-based contrast agents for magnetic resonance cancer imaging. *Wiley interdisciplinary reviews. Nanomedicine and nanobiotechnology* **2013**, *5* (1), 1−18.

(7) Petrini, I.; Barachini, S.; Carnicelli, V.; Galimberti, S.; Modeo, L.; Boni, R.; Sollini, M.; Erba, P. A. ED-B fibronectin expression is a marker of epithelial-mesenchymal transition in translational oncology. *Oncotarget* **2017**, *8* (3), 4914−4921.

(8) Han, Z.; Lu, Z. R. Targeting Fibronectin for Cancer Imaging and Therapy. *J. Mater. Chem. B* **2017**, *5* (4), 639−654.

(9) Freire-de-Lima, L.; Gelfenbeyn, K.; Ding, Y.; Mandel, U.; Clausen, H.; Handa, K.; Hakomori, S. I. Involvement of O-glycosylation defining oncofetal fibronectin in epithelial-mesenchymal transition process. *Proc. Natl. Acad. Sci. U. S. A.* **2011**, *108* (43), 17690−5.

(10) Han, Z.; Zhou, Z.; Shi, X.; Wang, J.; Wu, X.; Sun, D.; Chen, Y.; Zhu, H.; Magi-Galluzzi, C.; Lu, Z. R. EDB Fibronectin Specific Peptide for Prostate Cancer Targeting. *Bioconjugate Chem.* **2015**, *26* (5), 830−8.

(11) Lu, J.; Sabirianov, R. F.; Mei, W. N.; Gao, Y.; Duan, C. G.; Zeng, X. Structural and magnetic properties of Gd3N@C80. *J. Phys. Chem. B* **2006**, *110* (47), 23637−40.

(12) Li, Y.; Han, Z.; Roelle, S.; DeSanto, A.; Sabatelle, R.; Schur, R.; Lu, Z. R. Synthesis and Assessment of Peptide Gd-DOTA Conjugates Targeting Extradomain B Fibronectin for Magnetic Resonance Molecular Imaging of Prostate Cancer. *Mol. Pharmaceutics* **2017**, *14* (11), 3906−3915.

(13) Han, Z.; Li, Y.; Roelle, S.; Zhou, Z.; Liu, Y.; Sabatelle, R.; DeSanto, A.; Yu, X.; Zhu, H.; Magi-Galluzzi, C.; Lu, Z. R. Targeted Contrast Agent Specific to an Oncoprotein in Tumor Microenvironment with the Potential for Detection and Risk Stratification of Prostate Cancer with MRI. *Bioconjugate Chem.* **2017**, *28* (4), 1031−1040.

(14) Han, Z.; Wu, X.; Roelle, S.; Chen, C.; Schiemann, W. P.; Lu, Z. R. Author Correction: Targeted gadofullerene for sensitive magnetic resonance imaging and risk-stratification of breast cancer. *Nat. Commun.* **2018**, *9* (1), 153.

(15) Mastarone, D. J.; Harrison, V. S.; Eckermann, A. L.; Parigi, G.; Luchinat, C.; Meade, T. J. A modular system for the synthesis of multiplexed magnetic resonance probes. *J. Am. Chem. Soc.* **2011**, *133* (14), 5329−37.

(16) Fedorov, A.; Vangel, M. G.; Tempany, C. M.; Fennessy, F. M. Multiparametric Magnetic Resonance Imaging of the Prostate: Repeatability of Volume and Apparent Diffusion Coefficient Quantification. *Invest. Radiol.* **2017**, *52* (9), 538−546.

(17) Scheenen, T. W.; Rosenkrantz, A. B.; Haider, M. A.; Futterer, J. J. Multiparametric Magnetic Resonance Imaging in Prostate Cancer Management: Current Status and Future Perspectives. *Invest. Radiol.* **2015**, *50* (9), 594−600.

(18) Gleason, D. F. Histologic grading of prostate cancer: a perspective. *Hum. Pathol.* **1992**, *23* (3), 273−9.

(19) Glass, A. S.; Hilton, J. F.; Cowan, J. E.; Washington, S. L.; Carroll, P. R. Serial prostate biopsy and risk of lower urinary tract symptoms: results from a large, single-institution active surveillance cohort. *Urology* **2014**, *83* (1), 33−8.

(20) Vos, E. K.; Kobus, T.; Litjens, G. J.; Hambrock, T.; Hulsbergen-van de Kaa, C. A.; Barentsz, J. O.; Maas, M. C.; Scheenen, T. W. Multiparametric Magnetic Resonance Imaging for Discriminating Low-Grade From High-Grade Prostate Cancer. *Invest. Radiol.* **2015**, *50* (8), 490−7.

(21) Baur, A. D.; Maxeiner, A.; Franiel, T.; Kilic, E.; Huppertz, A.; Schwenke, C.; Hamm, B.; Durmus, T. Evaluation of the prostate imaging reporting and data system for the detection of prostate cancer by the results of targeted biopsy of the prostate. *Invest. Radiol.* **2014**, *49* (6), 411−20.

(22) Lim, E. K.; Kang, B.; Choi, Y.; Jang, E.; Han, S.; Lee, K.; Suh, J. S.; Haam, S.; Huh, Y. M. Gadolinium-based nanoparticles for highly efficient T1-weighted magnetic resonance imaging. *Nanotechnology* **2014**, *25* (24), 245103.

(23) Franano, F. N.; Edwards, W. B.; Welch, M. J.; Brechbiel, M. W.; Gansow, O. A.; Duncan, J. R. Biodistribution and metabolism of targeted and nontargeted protein-chelate-gadolinium complexes: evidence for gadolinium dissociation in vitro and in vivo. *Magn. Reson. Imaging* **1995**, *13* (2), 201−14.

DOI: 10.1021/acsmedchemlett.8b00172
ACS Med. Chem. Lett. 2018, 9, 730−735

(24) Sipkins, D. A.; Cheresh, D. A.; Kazemi, M. R.; Nevin, L. M.; Bednarski, M. D.; Li, K. C. Detection of tumor angiogenesis in vivo by alphaVbeta3-targeted magnetic resonance imaging. *Nat. Med.* **1998**, *4* (5), 623−6.
(25) Soulez, G.; Bloomgarden, D. C.; Rofsky, N. M.; Smith, M. P.; Abujudeh, H. H.; Morgan, D. E.; Lichtenstein, R. J.; Schiebler, M. L.; Wippold, F. J., 2nd; Russo, C.; Kuhn, M. J.; Mennitt, K. W.; Maki, J. H.; Stolpen, A.; Liou, J.; Semelka, R. C.; Kirchin, M. A.; Shen, N.; Pirovano, G.; Spinazzi, A. Prospective Cohort Study of Nephrogenic Systemic Fibrosis in Patients With Stage 3−5 Chronic Kidney Disease Undergoing MRI With Injected Gadobenate Dimeglumine or Gadoteridol. *AJR, Am. J. Roentgenol.* **2015**, *205* (3), 469−78.
(26) Idee, J. M.; Fretellier, N.; Robic, C.; Corot, C. The role of gadolinium chelates in the mechanism of nephrogenic systemic fibrosis: A critical update. *Crit. Rev. Toxicol.* **2014**, *44* (10), 895−913.
(27) Thomsen, H. S.; Marckmann, P. Extracellular Gd-CA: differences in prevalence of NSF. *Eur. J. Radiol.* **2008**, *66* (2), 180−3.
(28) Ye, F.; Wu, X.; Jeong, E. K.; Jia, Z.; Yang, T.; Parker, D.; Lu, Z. R. A peptide targeted contrast agent specific to fibrin-fibronectin complexes for cancer molecular imaging with MRI. *Bioconjugate Chem.* **2008**, *19* (12), 2300−3.
(29) Ye, F.; Jeong, K.-E.; Parker, D.; Lu, Z.-R. Evaluation of CLT1-(Gd-DTPA) for MR molecular imaging in a mouse breast cancer model. *Chin J. Magn Reson Imaging* **2011**, *2* (5), 376−381.
(30) White, G. W.; Gibby, W. A.; Tweedle, M. F. Comparison of Gd(DTPA-BMA) (Omniscan) versus Gd(HP-DO3A) (ProHance) relative to gadolinium retention in human bone tissue by inductively coupled plasma mass spectroscopy. *Invest. Radiol.* **2006**, *41* (3), 272−8.
(31) Morcos, S. K. Extracellular gadolinium contrast agents: differences in stability. *Eur. J. Radiol.* **2008**, *66* (2), 175−9.
(32) Lohrke, J.; Frisk, A. L.; Frenzel, T.; Schockel, L.; Rosenbruch, M.; Jost, G.; Lenhard, D. C.; Sieber, M. A.; Nischwitz, V.; Kuppers, A.; Pietsch, H. Histology and Gadolinium Distribution in the Rodent Brain After the Administration of Cumulative High Doses of Linear and Macrocyclic Gadolinium-Based Contrast Agents. *Invest. Radiol.* **2017**, *52* (6), 324−333.

DOI: 10.1021/acsmedchemlett.8b00172
ACS Med. Chem. Lett. 2018, 9, 730−735